

## Optical Activity of Oxo Amide Crystals

Toru Asahi,<sup>†</sup> Makoto Nakamura,<sup>†</sup> Jinzo Kobayashi,<sup>\*,†</sup> Fumio Toda,<sup>‡</sup> and Hisakazu Miyamoto<sup>‡</sup>

Contribution from the Kagami Memorial Laboratory for Materials Science and Technology, Waseda University, 2-8-26, Nishi-Waseda, Shinjuku-ku, Tokyo 169, Japan, and the Department of Applied Chemistry, Faculty of Engineering, Ehime University, Matsuyama, Ehime 790, Japan

Received June 14, 1996<sup>⊗</sup>

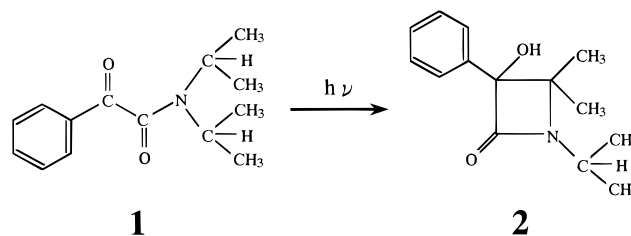
**Abstract:** It has been known that oxo amide crystals made up of achiral molecules can be photochemically converted into optically active  $\beta$ -lactams by irradiation with a high pressure mercury lamp. Although the oxo amide crystal belongs to an enantiomorphic class  $D_2$ , its optical activity could not be detected so far. We successfully measured the components of the gyration tensor of the oxo amide crystal by using the HAUP (high accuracy universal polarimeter) method:  $g_{11} = -3.5 \times 10^{-4}$  ( $-79^\circ/\text{mm}$ ),  $g_{22} = -1.4 \times 10^{-4}$  ( $-32^\circ/\text{mm}$ ),  $g_{33} = -3.0 \times 10^{-4}$  ( $-68^\circ/\text{mm}$ ) at 305 K, where the optical rotatory powers are indicated in parentheses. It has been proved by direct experiments that the optical activity of the reactant and the product in this reaction system remains unchanged over the photocyclization process.

## Introduction

Optical activity (OA)<sup>1</sup> of a noncentrosymmetrical molecule takes place when the displacement of some electron in the molecule is restricted to a helical path under the inhomogeneous electromagnetic field. Such a constraint to the helical path is caused by vicinal actions among the neighboring atoms in the molecule. It becomes possible<sup>2</sup> from the same reason that a crystal made up of achiral molecules becomes optically active when the degree of freedom of molecules, *e.g.*, rotation and orientation about chemical bonds, are severely restricted by forming a crystalline lattice. Quartz and diacetyl phenolphthalein<sup>2</sup> are typical examples, their crystalline states being optically active but immediately losing OA in liquid solutions.

Among optically active crystals composed of achiral molecules some crystals can be used as starting materials for absolute asymmetric synthesis of useful chemicals.<sup>3,4</sup> One of us (F.T)<sup>5</sup> successfully obtained optically active  $\beta$ -lactams 3-hydroxy-1-isopropyl-4,4-dimethyl-3-phenyl-azetidin-2-one (**2**), important antibiotics, by photocyclizations of optically active crystals of achiral oxo amide *N,N*-diisopropylphenylglyoxylamide (**1**) (Scheme 1). The space groups of both **1** and **2** crystals were established by X-ray structure analyses<sup>6</sup> as equally enantiomorphic  $D_2$ , which permits OA of both signs. Although the optical rotatory power of a solution of **2** was measured, *e.g.*,  $[\alpha]_D = +123^\circ$  (*c* 0.5 in  $\text{CHCl}_3$ ), OA of both crystals could not really be measured so far due to the presence of birefringence. Determinations of the absolute configurations of the structures of the reactant and the product were too difficult to be made, although recently those of *m*-chlorophenyl-*N,N*-

## Scheme 1



diisopropylglyoxylamide and the corresponding  $\beta$ -lactams were successfully determined.<sup>7</sup>

As there were no ways to determine OA of **1** crystal by using the existing methods, we<sup>5</sup> identified crystals of **1**, which gave **2**-crystals with (+) and (−) signs of OA in solutions, as (+)- and (−)-**1** respectively. However this identification is essentially tentative and presupposes that OA remains unchanged between the reactant and the product over the photochemical conversion. To be more general, such indeterminacy of OA of solids has been a long unresolved problem, which prevented accurate elucidation of the solid state asymmetric syntheses. We<sup>8–10</sup> developed the HAUP (high accuracy universal polarimeter) method, which enables us to measure simultaneously OA and birefringence  $\Delta n$  of crystals belonging to any systems. We applied the HAUP method to **1** crystals in order to investigate the above mentioned reaction more accurately.

## HAUP Measurement of Optical Activity

**1** crystals grown from benzene solution<sup>5</sup> were vitreous prisms, where (010) terrace planes were well developed. They were subjected to HAUP measurements. According to Weissenberg photographs of (−) and (+) specimens, the same lattice constants, say,  $a = 12.802$  (12.794) Å,  $b = 13.896$  (13.902) Å, and  $c = 7.487$  (7.506) Å, were obtained. They were in good

(7) Hashizume, D.; Kogo, H.; Sekine, A.; Ohashi, Y.; Miyamoto, H.; Toda, F. *J. Chem. Soc., Perkin Trans. 2* **1996**, 61.

(8) Kobayashi, J.; Uesu, Y. *J. Appl. Crystallogr.* **1983**, *16*, 204.

(9) Kobayashi, J.; Kumomi, H.; Saito, K. *J. Appl. Crystallogr.* **1986**, *19*, 377.

(10) Kobayashi, J.; Asahi, T.; Takahashi, S.; Glazer, A. M. *J. Appl. Crystallogr.* **1988**, *21*, 479.

<sup>†</sup> Waseda University.

<sup>‡</sup> Ehime University.

<sup>⊗</sup> Abstract published in *Advance ACS Abstracts*, April 1, 1997.

(1) Kobayashi, J. *Phys. Rev.* **1990**, *B42*, 8332.

(2) Kauzmann, W.; Eyring, H. *J. Chem. Phys.* **1941**, *9*, 41.

(3) Addadi, L.; van Mill, J.; Lahav, M. *J. Am. Chem. Soc.* **1982**, *104*, 3422.

(4) Evans, S.; Garcia-Garibay, M.; Omkaram, N.; Scheffer, J. R.; Trotter, J.; Wireko, F. *J. Am. Chem. Soc.* **1986**, *108*, 5648.

(5) Toda, F.; Yagi, M.; Soda, S. *J. Chem. Soc., Chem. Commun.* **1987**, 1413.

(6) Sekine, A.; Hori, K.; Ohashi, Y.; Yagi, M.; Toda, F. *J. Am. Chem. Soc.* **1989**, *111*, 697.

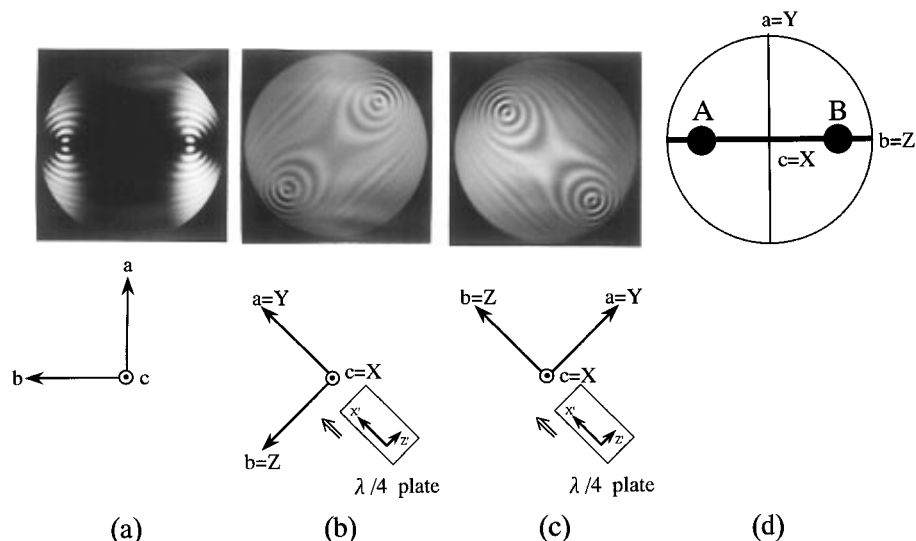


**Figure 1.** Conoscopic figures observed on (001) plane of **1** crystal: (a) indicates figure at an extinction position, (b) and (c) figures at 90° different diagonal positions, and (d) optical nature of the crystal.

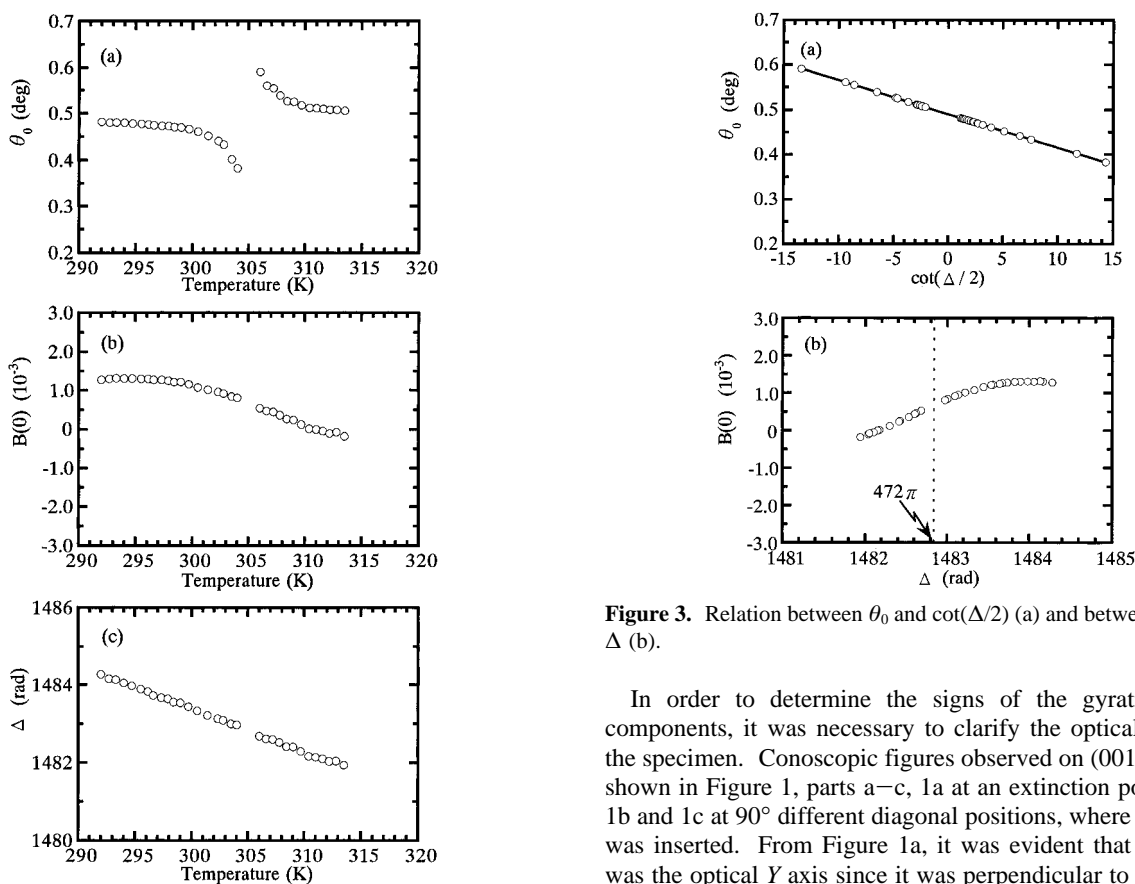


**Figure 2.** Temperature dependences of  $\theta_0$  (a),  $B(0)$  (b), and  $\Delta$  (c) of (100) plane of (-)1.

agreement with a previous report<sup>6</sup> (written in parentheses). Also the extinction rules of the reflections were consistent with the space group of  $D_2^4$ .

In order to avoid confusions in detecting the signs of OA of specimens, we made the HAUP measurements on (100), (010), and (001) planes of the same (-)1 specimen first. These planes were polished by fine (0.3  $\mu\text{m}$ )  $\text{Al}_2\text{O}_3$  powders. The lengths  $d$  of the intersections of the rectangular parallelepiped specimen were 813, 1256, and 1197  $\mu\text{m}$  along  $a$ ,  $b$ , and  $c$  axes, respectively. From the symmetry of this crystal, the gyrations  $G_1$ ,  $G_2$ , and  $G_3$  measured on (100), (010), and (001) planes equal gyration tensor components  $g_{11}$ ,  $g_{22}$ , and  $g_{33}$ , respectively.

**Figure 3.** Relation between  $\theta_0$  and  $\cot(\Delta/2)$  (a) and between  $B(0)$  and  $\Delta$  (b).

In order to determine the signs of the gyration tensor components, it was necessary to clarify the optical nature of the specimen. Conoscopic figures observed on (001) plane are shown in Figure 1, parts a–c, 1a at an extinction position and 1b and 1c at 90° different diagonal positions, where a  $\lambda/4$  plate was inserted. From Figure 1a, it was evident that the  $a$  axis was the optical  $Y$  axis since it was perpendicular to the optical plane, (100) plane. Birefringence increased when the  $b$  axis paralleled the  $Z'$  axis of the  $\lambda/4$  plate as shown in Figure 1b, while the reverse was the case in Figure 1c. Therefore the  $b$  axis must be the optical  $Z$  axis; the optical nature of the **1** crystal is expressed stereographically in Figure 1d.

In order to evaluate the linear dichroism of the specimen, the extended HAUP<sup>11</sup> method was used first in this experiment. However we found that it was less than  $1.3 \times 10^{-7}$  in any directions for the wavelength of 4965 Å (Ar laser). Therefore we could ignore it and used the simple method<sup>8</sup> in the following measurements. Temperature dependences of  $\theta_0$ ,  $B(0)$ , and  $\Delta$  of (100) specimen are shown in Figure 2. Here  $\Delta$  is the optical

(11) Kobayashi, J.; Asahi, T.; Sakurai, M.; Takahashi, M.; Okubo, K.; Enomoto, Y. *Phys. Rev.* **1996**, *B53*, 11784.

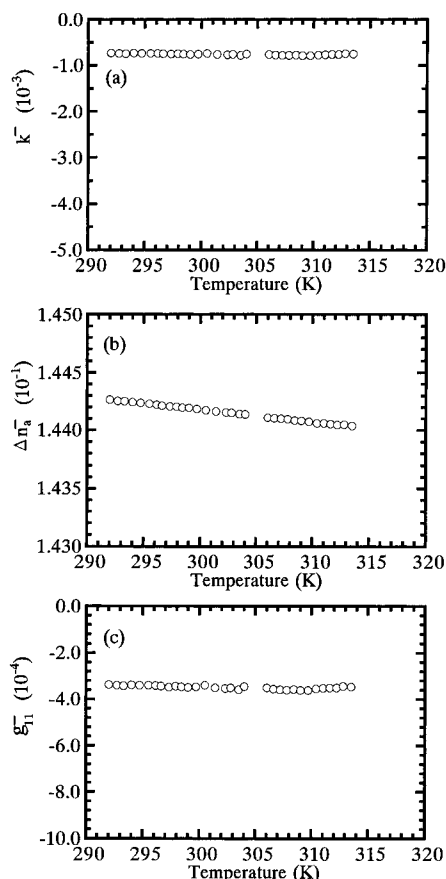


**Figure 4.** Temperature dependences of  $k^-$  (a),  $\Delta n_a^-$  (b), and  $g_{11}^-$  (c) of (100) plane of (-)-1.

**Table 1.** Systematic Errors and Thicknesses of Specimens of Oxo Amide

specimen	thickness( $\mu\text{m}$ )	systematic error			
		$p(10^{-4})$	$q(10^{-4})$	$\gamma(10^{-4})$	$\delta Y(10^{-4})$
(-)(1 0 0)	813	-1.5	4.1	-5.6	3.4
(-)(0 1 0)	1256	-1.5	-2.1	0.6	4.4
(-)(0 0 1)	1197	-1.5	2.3	-3.8	-1.0
(+)(0 0 1)	522	-1.5	32.6	-34.1	8.2

retardation, but  $\theta_0$  and  $B(0)$ , characteristic terms of the HAUP method, should be referred to refs 8 and 9. From these measurements the systematic errors<sup>8,9</sup>  $\gamma$  and  $\delta Y$  could be determined.  $\theta_0$  and  $B(0)$  are written as

$$\theta_0 = -\frac{1}{2}(p + q) \cot\left(\frac{\Delta}{2}\right) - \frac{1}{2}\delta Y \quad (1)$$

and

$$B(0) = (\gamma - 2k) \sin \Delta + 2\delta Y \cos^2\left(\frac{\Delta}{2}\right) \quad (2)$$

where  $\gamma = p - q$ ,  $p$  and  $q$  representing the parasitic ellipticities of the polarizer and analyzer, respectively.  $k$  stands for ellipticity. Relations between  $\theta_0$  and  $\cot(\Delta/2)$  and between  $B(0)$  and  $\Delta$  are indicated in Figure 3, parts a and b. From the derivative of  $\theta_0$  vs  $\cot(\Delta/2)$  in Figure 3a,  $p + q$  was determined to be  $2.6 \times 10^{-4}$ . Subsequently  $p$  could be determined to be  $-1.5 \times 10^{-4}$  by using a  $\text{LiNbO}_3$  crystal as the standard crystal,<sup>10</sup> but the description of the detailed procedure is omitted here. Therefore  $\gamma$  was evaluated to be  $-5.6 \times 10^{-4}$ .  $\delta Y$  was determined from the value of  $B(0)$  at  $\Delta = 472\pi$  in Figure 3b. As  $\gamma$  and  $\delta Y$  were thus determined, the ellipticity  $k$  could be

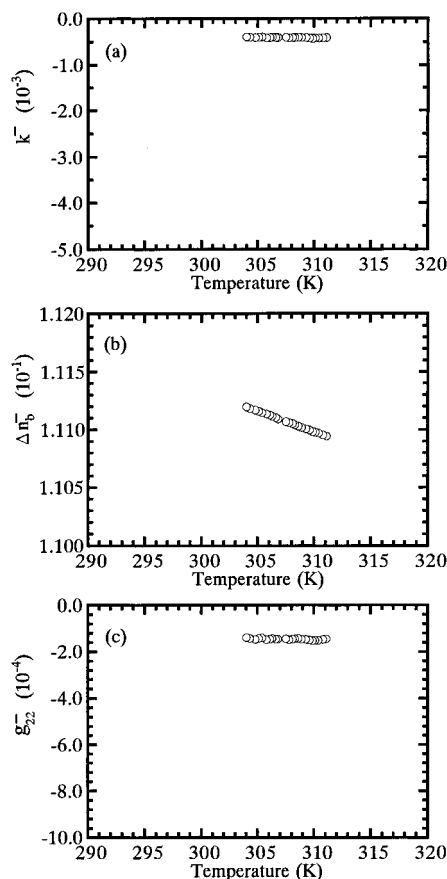


**Figure 5.** Temperature dependences of  $k^-$  (a),  $\Delta n_b^-$  (b), and  $g_{22}^-$  (c) of (010) plane of (-)-1.

**Table 2.** Optical Rotatory Powers of Crystals

crystal	$\lambda$ ( $\text{\AA}$ )	$T$ (K)	$\rho$ (deg $\text{mm}^{-1}$ )
$\text{AgGaS}_2$	4850		950 <sup>a</sup>
$\text{Ca}_2\text{Sr}(\text{C}_2\text{H}_5\text{COO})_6$	5890	293	4.2 <sup>b</sup>
$\alpha\text{-LiIO}_3$	6328		-86.7 <sup>c</sup>
$[\text{N}(\text{CH}_3)_4]_2\text{ZnCl}_4$	6328	292	0.02 <sup>d</sup>
$\alpha\text{-SiO}_2$	6328	293	25.1 <sup>e</sup>
$\text{TeO}_2$	6328		87 <sup>f</sup>
$\text{BaMnF}_4$	6328	133	5.7 <sup>g</sup>
$(\text{NH}_2\text{CH}_2\text{CO}_2\text{H})_3\text{H}_2\text{SO}_4$	6328	305	1.9 <sup>h</sup>
poly-L-lactic acid	5145	298	-9200 <sup>i</sup>
L-glutamic acid ( $\rho_3$ )	6328	293	5.4 <sup>j</sup>
oxo amide ( $\rho_1$ )	4965	305	-79
oxo amide ( $\rho_2$ )	4965	305	-32
oxo amide ( $\rho_3$ )	4965	305	-68

<sup>a</sup> Taken from ref 14. <sup>b</sup> Taken from ref 15. <sup>c</sup> Taken from ref 16. <sup>d</sup> Taken from ref 17. <sup>e</sup> Taken from ref 10. <sup>f</sup> Taken from ref 18. <sup>g</sup> Taken from ref 19. <sup>h</sup> Taken from ref 20. <sup>i</sup> Taken from ref 21. <sup>j</sup> Taken from ref 22.

evaluated from (2).  $\Delta n$  was calculated from the relation

$$\Delta = \frac{2\pi}{\lambda} \Delta n d \quad (3)$$

where  $\lambda$  expresses the wavelength of the incident light.  $G$  can be obtained from the relation

$$k = \frac{G}{2\Delta n \bar{n}} \quad (4)$$

where  $\bar{n}$  represents the mean refractive index. It was determined to be 1.61 by using Chaulnes' method.<sup>12</sup> Temperature depend-

(12) Wahlstrom, E. E. *Optical Crystallography*; John Wiley: New York, 1951; p 66.

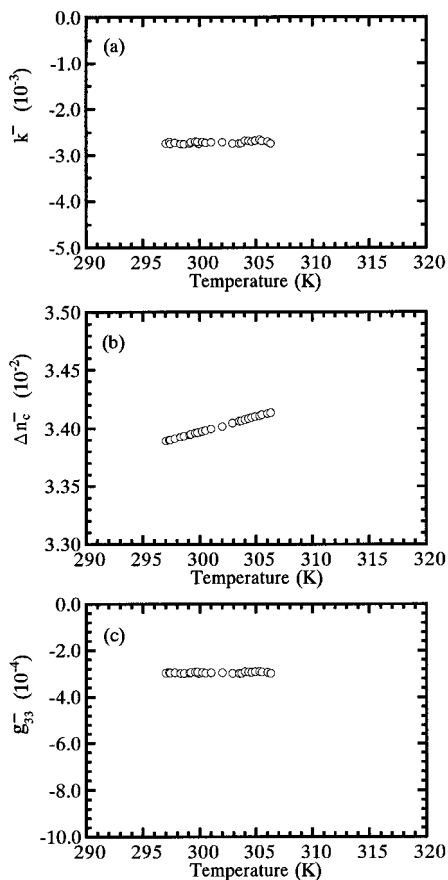


**Figure 6.** Temperature dependences of  $k^-$  (a),  $\Delta n_c^-$  (b), and  $g_{33}^-$  (c) of (001) plane of (-)-1.

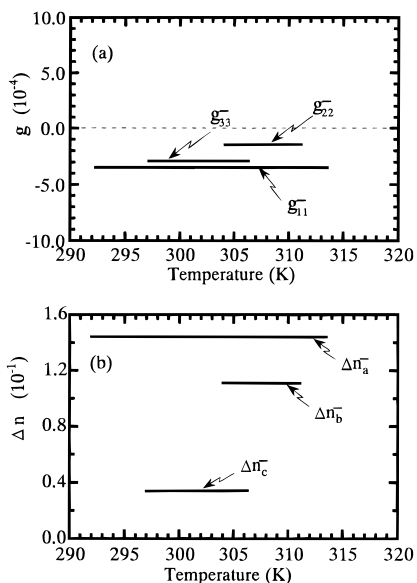


**Figure 7.** Temperature dependences of all the components of the gyration tensor (a) and birefringences (b) of (-)-1.

ences of  $k^-$ ,  $\Delta n_a^-$ , and  $G_1^- (= g_{11}^-)$  were clarified as shown in Figure 4, parts a–c, where a superscript – designates (–)-crystal.  $g_{11}^-$  is about  $-3.5 \times 10^{-4}$ , and independent of temperature.  $\Delta n_a^-$ , which is approximately the same magnitude as calcite, manifests the negative temperature coefficient.

Analogous measurements were performed on (010) and (001) planes. Systematic errors  $\gamma$  and  $\delta Y$  of these cases are indicated in Table 1 together with thicknesses. Temperature dependences of  $k$ ,  $\Delta n$ , and  $g$  of (010) and (001) planes are depicted in Figures 5 and 6. Both  $g_{22}^-$  and  $g_{33}^-$  are also negative and independent of

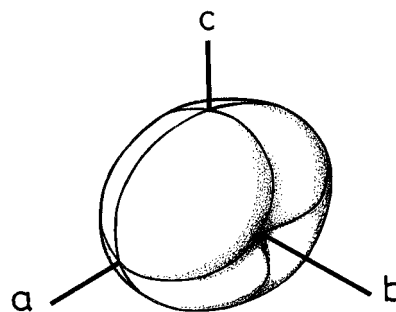


**Figure 8.** Gyration surface of (-)-1.

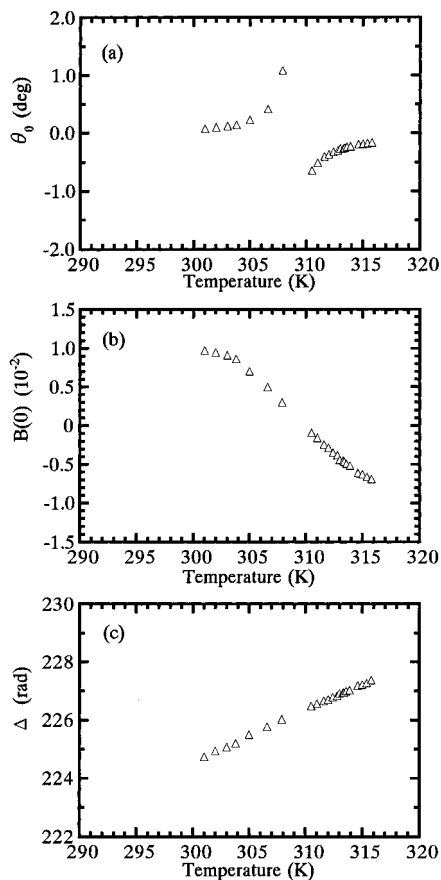


**Figure 9.** Temperature dependences of  $\theta_0$  (a),  $B(0)$  (b), and  $\Delta$  (c) of (001) plane of (+)-1.

temperature. It is noticeable that  $\Delta n_c^-$  is one order of magnitude lower than the others and increases with increasing temperatures. Temperature dependences of all the components of the gyration tensor and birefringence are summarized in Figure 7, parts a and b. It was found that the components of the gyration tensors of (-)-1 crystal are negative and remain almost constant in the present temperature range. The gyration surface<sup>13</sup> of this crystal is a white ovoid as shown in Figure 8. It is seen from the figure that there are no directions where positive gyrations can occur in the crystal.

As for OA of (+)-1 crystal, a (001) plate specimen were prepared with an area of  $2000 \times 3500 \mu\text{m}^2$  and a thickness of

(13) Shubnikov, V. A. *Principles of Optical Crystallography*; Consultant Bureau: New York, 1960; p 111.

(14) Hobden, M. V. *Nature* **1967**, 216, 678.

(15) Kobayashi, J.; Bouillot, J.; Kinoshita, K. *Phys. Status Solidi B* **1971**, 47, 619.

(16) Stadnicka, K.; Glazer, A. M.; Moxon, J. R. L. *J. Appl. Crystallogr.* **1985**, 18, 237.

(17) Kobayashi, J.; Saito, K.; Takahashi, N.; Kamiya, I. *Phys. Rev.* **1993**, B48, 10038.

(18) McCarthy, K. A.; Goutzoulis, A. P.; Gottlieb, M.; Singh, N. B. *Opt. Commun.* **1987**, 64, 157.

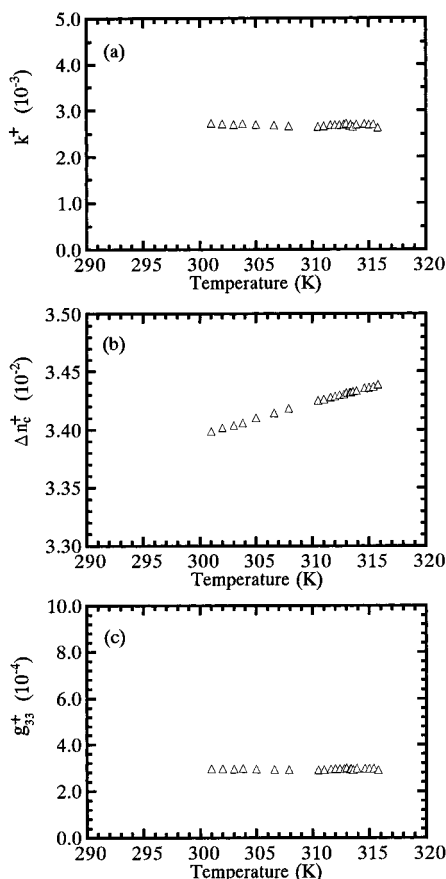


**Figure 10.** Temperature dependences of  $k^+$  (a),  $\Delta n_c^+$  (b), and  $g_{33}^+$  (c) of (001) plane of (+)-1.

522  $\mu\text{m}$ . Temperature dependences of  $\theta_0$ ,  $B(0)$ , and  $\Delta$  are shown in Figure 9, parts a–c. The systematic errors were determined as  $\gamma = -3.41 \times 10^{-3}$  and  $\delta Y = 8.2 \times 10^{-4}$ . Temperature dependences of  $k^+$ ,  $\Delta n_c^+$ , and  $G_3^+$  ( $= g_{33}^+$ ) are represented in Figure 10, parts a–c. Temperature dependences of  $\Delta n_c^\pm$ , and  $g_{33}^\pm$  of both specimens are compared in Figure 11, parts a and b.  $\Delta n_c^-$  and  $\Delta n_c^+$  of both crystals constitute the same straight line. This fact shows the coincidence of  $\Delta n$  of both crystals and indicates the validity of the present experiments.  $g_{33}^-$  and  $g_{33}^+$  are juxtaposed at the same levels but with opposite signs.

We omitted to measure OA on (100) and (010) planes of (+)-1 crystal, since there was no question that tensor compo-

(19) Asahi, T.; Tomizawa, M.; Kobayashi, J.; Kleemann, W. *Phys. Rev.* **1992**, *B45*, 1971.

(20) Kobayashi, J.; Uchino, K.; Matsuyama, H.; Saito, K. *J. Appl. Phys.* **1991**, *69*, 409.

(21) Kobayashi, J.; Asahi, T.; Ichiki, M.; Oikawa, A.; Suzuki, H.; Watanabe, T.; Fukada, E.; Shikinami, Y. *J. Appl. Phys.* **1995**, *77*, 2957.

(22) Asahi, T.; Utsumi, H.; Itagaki, Y.; Kagomiya, I.; Kobayashi, J. *Acta Crystallogr., Sect. A* **1996**, *52*, 766.

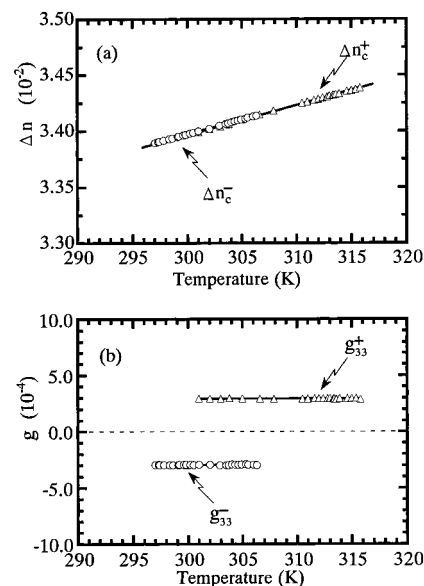


**Figure 11.** Comparisons of temperature dependences of  $\Delta n_c^-$  and  $\Delta n_c^+$  (a) and  $g_{33}^-$  and  $g_{33}^+$  (b).

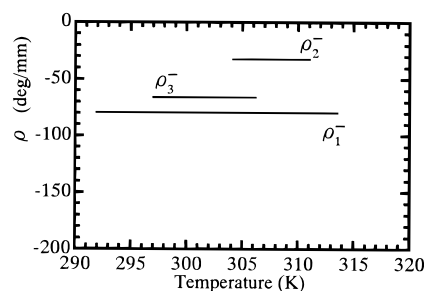


**Figure 12.** Temperature dependences of optical rotatory powers  $\rho_1^-$ ,  $\rho_2^-$ , and  $\rho_3^-$  of (-)-1.

nents  $g_{11}^+$  and  $g_{22}^+$  would have the same magnitudes of opposite signs as the corresponding components of (-)-1. Temperature dependences of the optical rotatory powers  $\rho_1^-$ ,  $\rho_2^-$ , and  $\rho_3^-$  of (-)-1 are depicted in Figure 12. Also they are compared with other crystals in Table 2. It is seen that the optical rotatory powers of 1 are larger than that of quartz,  $\rho_1^-$  and  $\rho_3^-$  being approximately three times larger.

Summing up the present paper, we have proved quantitatively that oxo amide crystals which give (-)- and (+)- $\beta$ -lactams really manifest negative and positive OA. Thus the serious problem in solid state asymmetric syntheses, say, indeterminacy of OA of solids, has been solved by using the HAUP method.

**Acknowledgment.** This paper is dedicated to Professor Nelson J. Leonard on the occasion of his 80th birthday.

JA9620189